Australian Journal of Basic and Applied Sciences, 6(6): 309-322, 2012
ISSN 1991-8178

Diagenesis and Petrophysical Properties of the Middle Miocene (Belayim Formation) at Belayim Land Oil Field, West Sinai, Egypt.

Ramadan, F.S. and Eysa, E.A.

Geology Department, Faculty of Science, Zagazig University

Abstract: The sandstones of Belayim Formation form an important hydrocarbon reservoir in south west Sinai. A study of the diagenetic evolution of Belayim sandstones in the Bell Bay – 4 well was undertaken to unravel the controls on reservoir quality and to study sequential diagenetic changes. Core samples were selected from Bell Bay – 4 well with depth ranges from 2487m to 2609 m. It represents fine to coarse grained, angular to subrounded and moderately to poorly sorted sandstone. The detrital constituents of the Middle Miocene sandstones are dominated by quartz, feldspar and subordinated lithic fragments and micas. Cement types include Fe-calcite, quartz overgrowths, ferroan dolomite, siderite and k-feldspar overgrowths. Six microfacies types are recorded namely: sideritic subfeldspathic arenite, sideritic quartz arenite, subfeldspathic arenite, sideritic sublithic arenite, sublithic arenite and dolomitic sublithic arenite. The carbonates cementation, quartz overgrowths, dolomitization, mechanical and chemical compaction played an important role of porosity loss in some of the examined samples in the studied formation. Diagenetic and related reservoir properties evolutions of the Middle Miocene sand stoes have been excuated during eo- and meso diagenesis. The petrophysical characteristics of the rocks showed that, the sandstones in the Belayim Formation have a high porosity (good to very good) and good to excellent permeability and thus, have a good storage capacity and reservoir quality. The distribution of porosity and permeability values reflects the heterogeneity. The high permeability values, both horizontal and vertical, with relative increasing in horizontal than vertical permeability indicate good reservoir characteristics. The porosity is strongly correlated reversely with pressure and the most of pore radii are ranging from 0.3 μm to 10 μm which permit different types of fluid to pass easily indicating high quality reservoir.

Key words: Diagenesis, Petrophysics, Belayim, Miocene, Sinai and Egypt.

INTRODUCTION

The Gulf of Suez is the most important oil-producing region in Egypt and accounts for more than 75% of Egyptian oil production (EGPC, 1996).

The Gulf of Suez forms the north-western arm of the Red Sea rift system and separates the Sinai Peninsula from the remainder of Egypt. It is a Cenozoic rift having 300 Km long and up to 80 Km wide. Be1ayim oil fields are located on the eastern side of the Gulf of Suez, one hundred and sixty five kilometers southeast of the Suez city. The Gulf is nearly bounded by Latitudes 27 º 41' N - 30 º 00' N and Longitudes 32 º 22' E - 34 º 10' E. Two oil fields are known, The Belayim land and The Belayim marine oil fields. Study area focuses on the eastern flank of Belayim land oil field (Fig.1).

The available data include ten core samples and core analysis reports for Belayim Formation in well Bell Bay – 4 which are used for evaluating the diagenetic process and petrophysical parameters of Belayim Formation. The used data are licensed from Egyptian General Petroleum Corporation (EGPC) and obtained from Belayim Petroleum Company (Petrobel).

Geological Setting:

The common structural evolution of the Gulf of Suez and the Red Sea began in Oligocene - Miocene times. Geomorphologically, the Gulf of Suez can be described as a rejuvenated, slightly acute NW - SE trending depression. It separates Sinai massif from the Eastern Desert - Red Sea hills and referred to as the clysmic Gulf. Because of the importance of the Gulf of Suez as the main oil producing province in Egypt, Many authors dealt with its geology, stratigraphy, structure and geological history.

The Miocene section consists of two main groups (Ghorab, 1964; El-Gezeery and Marzouk, 1974 and Darwish and Araby, 1993). The lower group is the Early Miocene clastics (Gharandal Group) and having the Nukhul, Rudeis and Kareem formations. This followed by Middle Miocene evaporites (Ras Malaab Group) as upper group which consists of Belayim, South Gharib and Zeit formations (Fig. 2).

The Belayim Formation represents the marine Miocene evaporite cycle, it deposited in NW - SE trending low areas. Belayim deposits consist mainly of evaporites (anhydrites and salts), shales, limestones and

Corresponding Author: Ramadan, F.S., Geology Department, Faculty of Science, Zagazig University

sandstones. This indicates littoral and lagoonal conditions of deposition. The Belayim sandstone constitutes a good hydrocarbon reservoir in several oil fields in the central and southern Gulf of Suez.

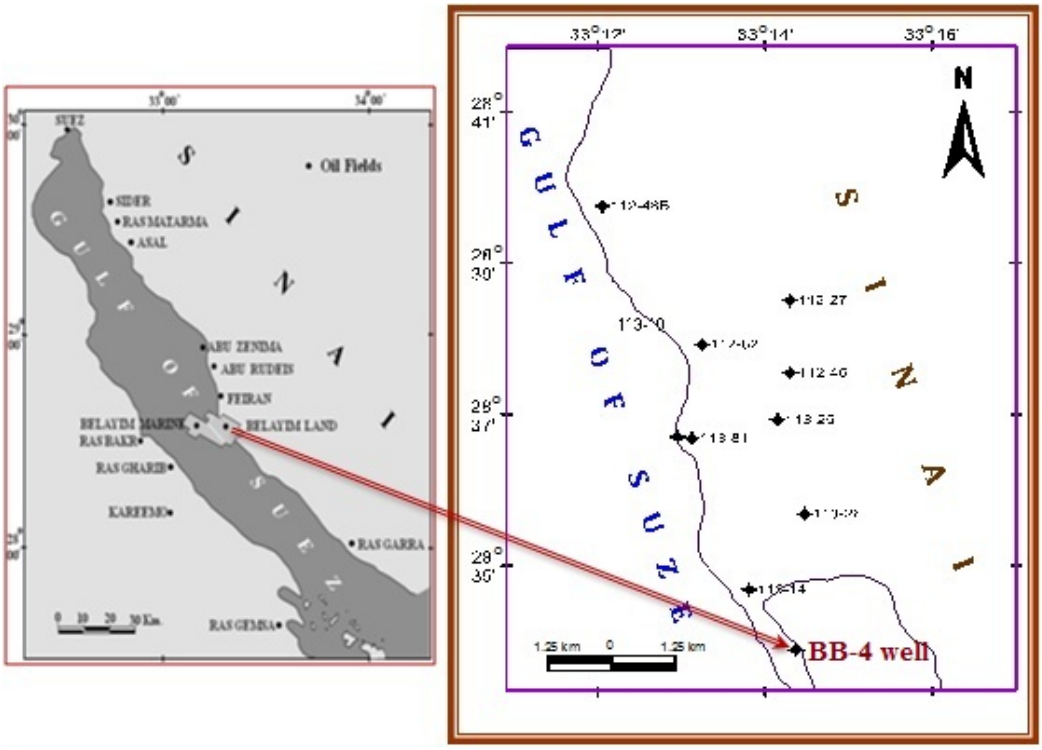

Fig. 1: Location map of Well Bell Bay-4 in belayim land oil field, West Sinai, Egypt.

Methodology:

Ten core samples were chosen to represent the Belayim sandstone in the studied well. Texture and mineralogical composition were studied using polarized light microscopy, scanning electron microscope (SEM) and X- ray diffraction analyses (XRD).

Twenty thin sections were prepared to determine their mineral composition, microfacies associations and diagenetic processes. Their preparation involved vacuum impregnation with blue dyed resin to facilitate the recognition of porosity, and stained with a mixed Alizarin Red-S and potassium ferricyanide solutions to identify the carbonate solution to aid the recognition of alkali feldspar. Each thin section was point-counted (200 points). Eight samples of different lithofacies were examined by Scanning Electron Microscope Model Philips X30. XRD analysis was carried out on four core samples.

The petrophysical properties of the rock including porosity, permeability, pore radii and effect of pressure were studied, analysed and plotted using reports of conventional and special core analysis. The porosity and permeability are classified according to Levorsen (1967).

RESULTS AND DISCUSSION

Composition of Sandstones:

The studied sandstones are fine- to coarse-grained, moderately to poorly sorted. The grains are angular to subrounded. Figure (3) represents the distribution of detrital and authogenic minerals in the studied samples. According to the Pettijohn *et al.* classification's (1972), the study of the microfacies associations in the Belayim Formation in well Bell Bay – 4 revealed the presence of six microfacies types namely: sideritic subfeldspathic arenite, sideritic quartz arenite, subfeldspathic arenite, sideritic sublithic arenite, sublithic arenite and dolomitic sublithic arenite (Fig. 4). Quartz represents the main compoent of grain framework, the content of which ranges from 36 to 45 vol%. The monocrystalline quartz predominates over the polycrystalline quartz, which includes fragments of cherts (average about 3 vol%). Small quartz grains are mostly angular, while grains of the coarse fraction are characterized by a better roundness. The contact between quartz grains evidenced by concavo-convex and tangential grain-grain contacts (Fig. 5A).

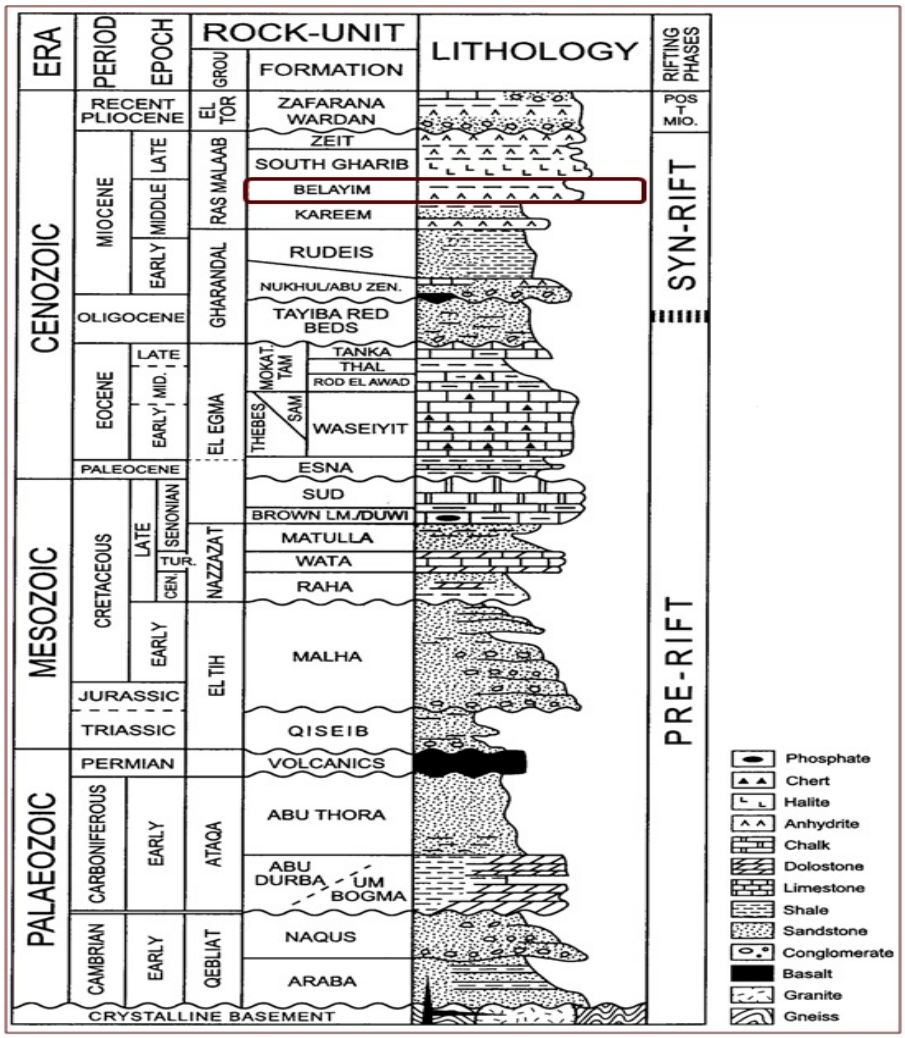

Fig. 2: Generalized lithostratigraphic column of the Gulf of Suez (after Darwish and El-Araby 1993).

Feldspars occur in all analysed sandstone samples in an amount from 0.5 to 4.5 vol%. There are mainly potassium feldspars, represented by microcline and orthoclase (Fig. 3A). Sodium-calcium plagioclase appears less frequent. Some feldspar grains have been partially or completely replaced by calcite (Fig. 5B).

The lithic fragments are a common component of sandstones, and their content varies from 1.5 to 8.5 vol%. The fragments of sedimentary rocks are mainly of limestone, rarely claystones, siltstones and sandstones. Fragments of metamorphic rocks are (0–3 vol%), represented by mica and quartz-mica schists.

Micas occur in various amounts (0.5–3 vol%), with a muscovite predominance over biotite. Calcite bioclasts were observed in similar quantities in the analysed sandstones, from 0 to 2.5 vol%. The other components of content less than 1 vol% in sandstone are: organic matter, heavy minerals (mainly zircon and apatite) and glauconite. Glauconite forms oval, green grains of various sizes that are affected by varying degrees of chloritization and pyritization (Fig. 5B & C).

Partially, secondary porosity resulted from dissolution of mica grains and formation of kaolinite at the expense of micas is noticed (Fig. 5E).

Matrix is composed of a mixture of clay minerals, quartz dust, iron hydroxides and muds, the content of which locally reaches10 vol% (Fig. 5D & 6A).

XRD analyses of clay minerals showed the presence variable content of kaolinite. Mainly carbonate minerals and less quartz and clay minerals form the cement in the studied sandstones. Pyrite occurs in an amount from 0.5 to 2.5 vol%. Ferroandolomite appears in an amount from 0.0 to 26 vol% (Fig. 6B). Siderite recorded in an amount from 1.5 to 23 vol%. (Figs. 3B, 5D & 6C).

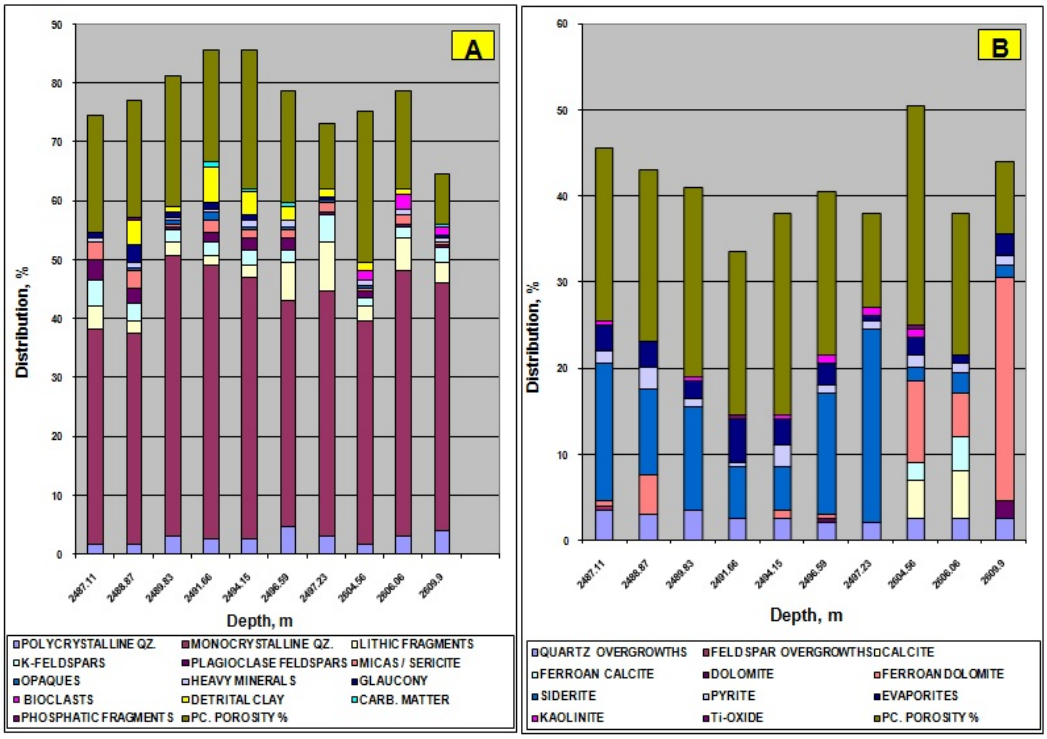

Fig. 3: Distribution of major detrital (A) and authogenic components (B) and point counted porosity in BB-4 well.

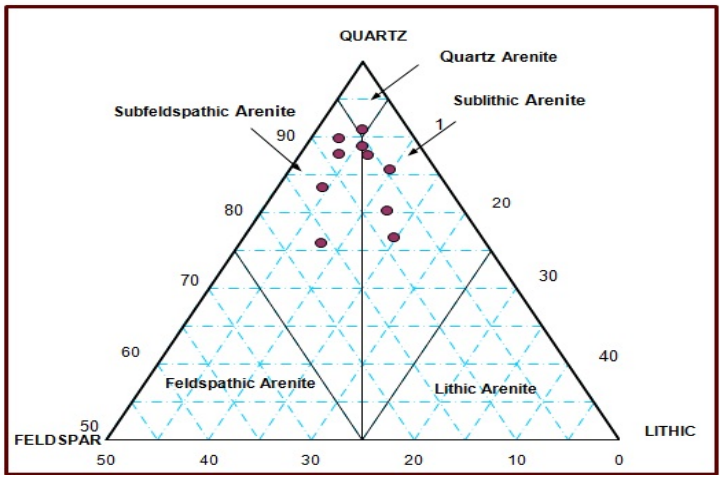

Fig. 4: QFL sandstone triangular composition plot, Belayim Fm., BB-4 well.

Diagenetic Minerals:

Carbonate cements are mostly calcite and subordinately dolomite and siderite. Two calcite cement generations are present. Micritic calcite precipitated on the surface of grains and in primary pores is the first generation. Sparite or poikilotopic calcite which precipitated in primary and secondary pore space in sandstones is the second generation (Fig. 6D). The content of calcite cements is unequal and varies from 0 to over 5.5 vol% (Fig. 3B). Calcite replaces feldspar grains and rock fragments often forming pseudomorphs (Fig. 6C). Poikilotopic calcite surrounds and hence postdates quartz overgrowth and dolomite rhombohedrons (Fig. 6D).

Dolomite occurs in the sandstones as pore filling rhombohedrons (Fig. 6B). Some of crystals show zonation with a core containing less Fe than rims (Fig. 6D). The dolomite crystals are surrounded by Fe-calcite, the ferroan dolomite increased at depth 2609.9 to reach 26 vol% with considerable porosity reduction. Siderite

occurs as scattered microcrystalline crystals in the sandstones, it ranges from 1.5 to 23 vol%, the maximum value at depth 2497.23m is contemporaneous with observed reduction in porosity (Fig. 3B).

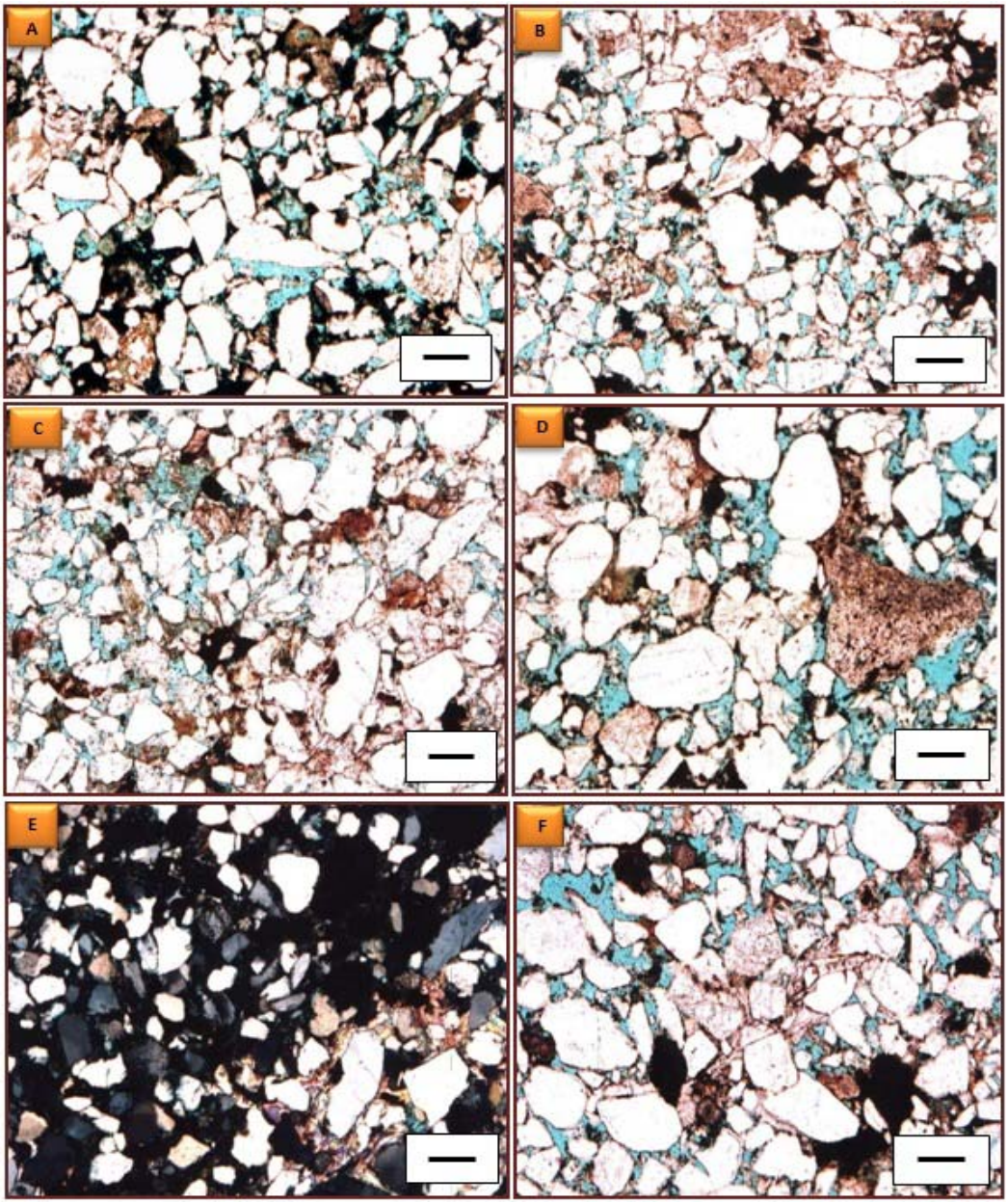

Fig. 5: Photographs in polarizing microscope A. Contact between quartz grains; concavo-convex and tangential grain-grain contacts depth 2,487.11m, PL. B. Feldspar grains have been partially or completely replaced by calcite 2,488.87 m. C. poor porosity, galuconite forms oval, green grains of various size and compaction reduced pore space, depth 2491.66 m. D. Quartz overgrowths, detrital clay and siderite, depth 2489.83, PL. E. Secondary porosity resulted from dissolution of mica grains and formation of kaolinite at the expense of micas, depth 2,494.15 m, CN F., Contact between quartz grains and dolomite cement, depth 2,494.15m, PL. Bare scale=260 microns.

Authigenic clay minerals observed under the polarizing microscope and scanning electron microscope (SEM) are kaolinite. Kaolinite occurs as booklets and vermicular stacked pseudohexagonal crystals (Fig.7A). Most studied samples have good porosity between quartz grains and kaolinitic matrix (Fig. 7B). Vermicular kaolinite is locally distributed in intergranular and intragranular space of the Middle Miocene sandstone. Kaolinite is surrounded by quartz overgrowths and hence it pre-dates the quartz. Occasionally, kaolinite locally

replaces detrital feldspar and muscovite (Fig. 5E & 7C). Quartz overgrowth is oriented in the same crystallographic direction (Fig. 7D).

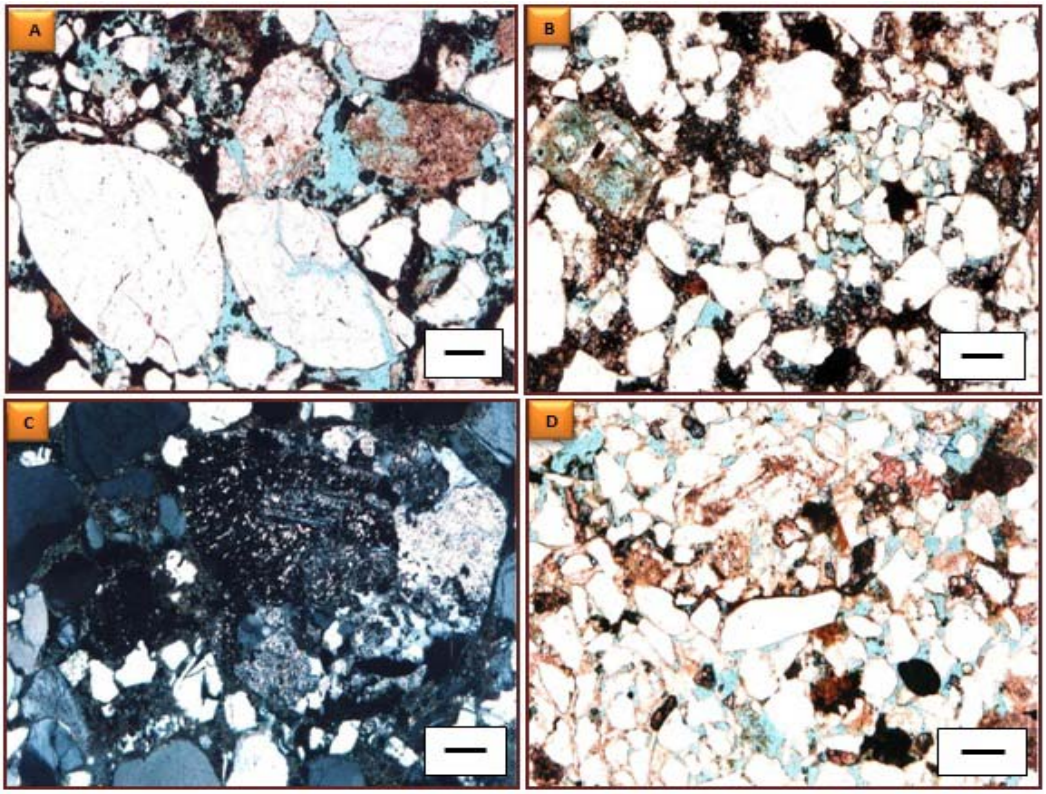

Fig. 6: Photographs in polarizing microscope A. Quartz grains are medium to coarse, sub-rounded to rounded, moderately to well-sorted, matrix of fine quartz grains and Secondary porosity depth 2497.23m, PL. B. Pore space between quartz grains reduced by ferroan dolomite rhombic, depth 2609.90 m, PL. C. Secondary porosity resulted from dissolution of feldspar and lithoclast grain, partially siderite reduced pores, depth 2497.23m, PL. D. Calcite cement partially replaced quartz overgrowths on quartz grain depth 2604.56m, CN bare scale=260 microns.

The quartz cement is commonly less than 2 vol% of the whole rock and rarely reaches 3.5 vol%. It occurs as partial to complete syntaxial overgrowths around the quartz grains. The boundary between the overgrowths and the detrital core is either poorly defined or delineated by fluid inclusions or thin clay coatings. It is not easy to discriminate quartz overgrowth from detrital grains in thin sections in microscope. In SEM images, authigenic quartz overgrowths are very well visible as rhombohedral crystals and prisms on detrital quartz grains (Figs.7D, E & F). Quartz cement is replaced by calcite (Fig. 6D) and locally covered by dolomite (Figs. 7C & H).

Minor diagenetic minerals include feldspars and pyrite. Sometimes, feldspars with developed cleavages and detrital clay filling sandstone pore space (Fig. 7E). Pyrite occurs as scattered framboids filling primary and secondary pores in the rocks (Fig. 7G). Authigenic feldspars occur as K-feldspar overgrowths on partly to completely sericitized plagioclase grains (Fig. 7F). The K-feldspar overgrowths are surrounded by, and hence predate, quartz overgrowths that have been developed on the adjacent quartz grains. Figures (3A & B) represent the distribution of detrital and authgenic minerals in the studied samples.

Porosity and Permability:

The porosity measured in thin sections ranges from 8.5 to 26 vol%. According to Jenyon's (1990) classification, the Middle Miocene sandstones can be concerned as the rocks of a good porosity. Both primary and secondary pore types are present in the sandstones. Primary intergranular pores are the abundant pores and are affected by compaction and cementation (Figs. 5B & C). Secondary intragranular pores were primarily associated with the dissolution of detrital feldspars and lithic fragments and calcite cement (Figs. 5E & 6C.). Some of the secondary pores are inside the quartz grains (Fig. 6A). Intercrystalline porosity in clay aggregates (micropores) was associated with the presence of clays.

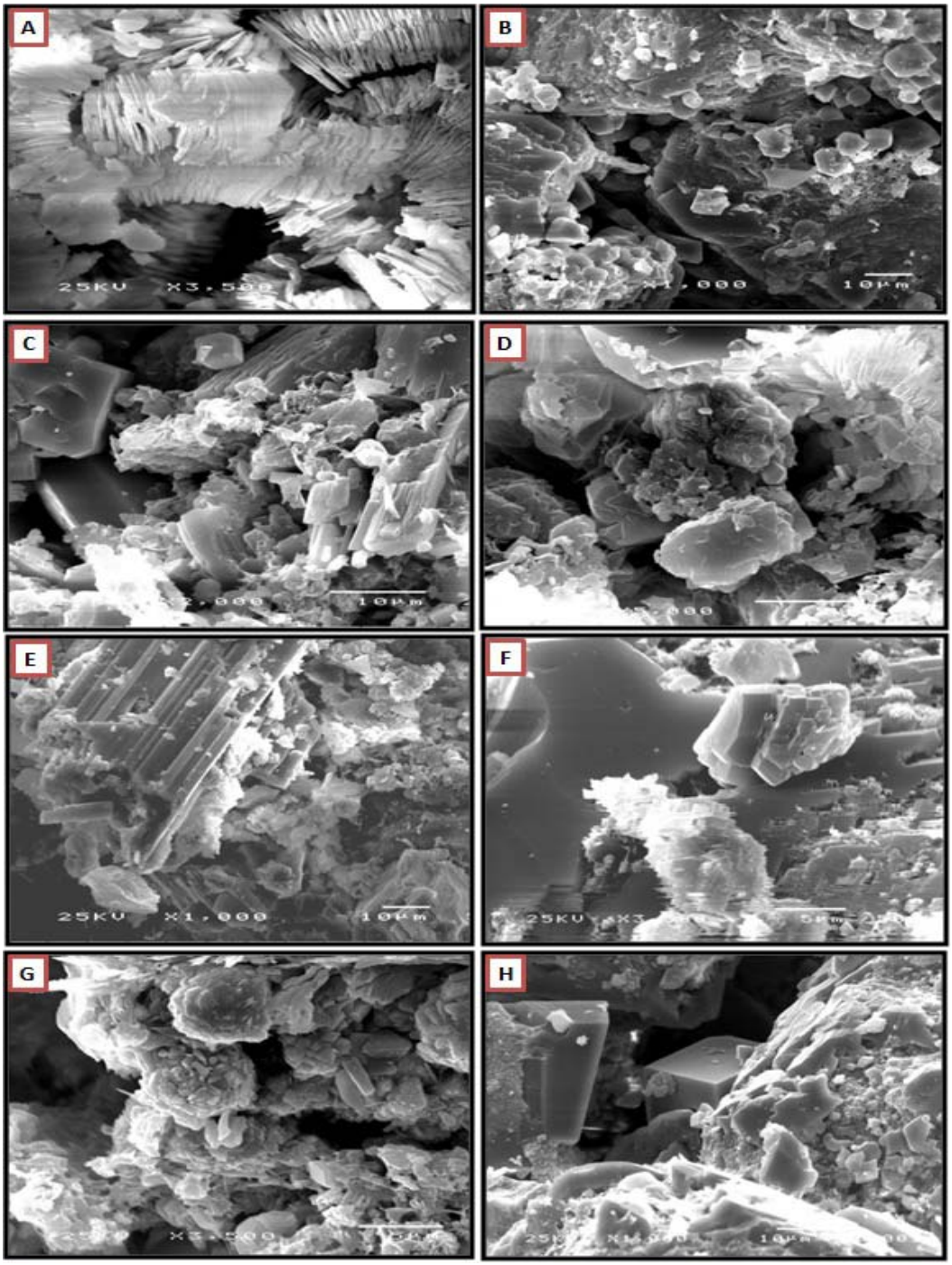

Fig. 7: Scanning electron microcope (SEM) photographs. A. Curved vermicular stacks, characteristic structure of kaolinite, depth 2487.11m. B. Good porosity between quartz grains and kaolinitic matrix, depth 2488.87m. C. Authigenic dolomite (euhedral rhombic outline), feldspars and clays in sandstone, 2488.87m. D. Quartz overgrowth are oriented in the same crystallographic direction, depth 2489.83m. E. Feldspars with developed cleavages and filled intergranular pore space, depth 2496.59m.G. Pyrite framboids in pore space of sandstone, depth 2497.23m. H. Considerable porosity between quartz grains although partially reduced by rhombic ferroan dolomite, depth 2609.90m.

Petrophysial Properties:

Conventional core analysis is a very important part of an overall reservoir assessment. It enables direct evaluation of reservoir properties and provides a basis to collaborate other evaluation tools such as logs. In this

study, we are used the data of 116 core samples of Belayim Formation in the core report of Bell Bay – 4 well. The report includes measurements of helium porosity (ϕ_h), horizontal and vertical permeability (K_h, K_v). In this study, some relationships and statistical analysis for porosity and permeability types are computed.

The porosity of a rock is one of the most important properties because it controls the storage capacity of the reservoir. The porosity of a rock sample is defined as the percentage ratio of the void space to the bulk volume. It can be expressed in a mathematical form as:

$$\phi = \frac{Vb - Vgr}{Vb} = \frac{Vp}{Vb} = \frac{Vp}{Vp + Vgr} \quad (1)$$

Where: ϕ = porosity (fraction), Vb = bulk volume of the reservoir rock,
Vgr = grain volume and Vp = pore volume.

Levorsen, 1967 classified the reservoir porosity into five categories, negligible from 0-5%, poor from 5-10%, fair from 10-15%, good from 15-20% and very good from 20-25%.

Table (1) represents the descriptive statistical analysis for porosity and permeability data of the analyzed samples. It can be observed that, the helium porosity of Belayim Formation in Bell Bay – 4 well varies from 2.2% to 25.8%. The calculated mean, median and standard deviation are 14.8, 16.3 and 7.1 respectively. The standard deviations indicate that, the porosity of Belayim Formation is heterogeneous.

Table 1: Descriptive statistical analysis of porosity and permeability types of Belayim Fm., BB-4 well.

Descriptive statistical	Horizontal Permeability (K_h), md	Vertical Permeability (K_v), md	Helium Porosity (Φ_h)
Mean	114.2	104.5	14.8
Median	24.9	18.8	16.3
Mode	1.1	0.7	17.0
Standard Deviation	232.7	228.3	7.1
Minimum	0.2	0.1	2.2
Maximum	1196.7	1158.8	25.8
Sun	13244.7	12123.2	1718.7
Count	116	116	116.0

Fm: Formation

The porosity histogram and cumulative frequency for the studied samples are shown in figure (8) which shows that, 28.45% and 25.86% of the samples have represented by good and very good quality, respectively.

Permeability is the ability of the rock to conduct fluids through it under a certain pressure gradient (measured in millidarcy). Permeability is quantitatively defined by an empirical relation known as Darcy law:

$$K = \frac{Q\mu}{A}\frac{L}{\Delta P} \quad (2)$$

Where: K = permeability, Darcy's; Q = volume flow rate, cc/sec;
μ = fluid viscosity, centipoises; L = length of the rock sample, cm;
A = cross sectional area of rock sample, cm^2; P = pressure drop, atmosphere.

The quality of a reservoir depends on the permeability values where it can be divided into four types: fair (1-10 md), good (10-100 md), very good (100-1000 md) and excellent (>1000 md) (Levorsen, 1967).

The summary of descriptive statistical analysis for permeability data of the studied samples is shown in Table (1). Vertical and horizontal permeability ranges from 0.2 to 1196.7and from 0.1 to 1158.8 md with averages of 114.2 and 104.5 md. The values of mean, median, mode and standard deviation for both horizontal and vertical permeabilities reflect the heterogeneity of the permeability values. The statistical analysis of the permeability shows that, the values of horizontal permeability exceed those of vertical permeability, which means a high quality reservoir. The permeability histograms and cumulative frequency for the studied samples are shown in figures (9 and 10). In the horizontal permeability, 27.58 %, 37.07 %, 22.42 % and 1.72 % of the samples represented by fair, good, very good and excellent reservoir respectively. In the vertical permeability of the same samples, 19.83 %, 35.35 %, 19.82 % and 2.59 % of the samples represent by fair, good, very good and excellent reservoir. More than 61 % of the samples, in case of horizontal permeability, represented by good to excellent reservoir, while more than 57% of the samples, in case of vertical permeability, are a good to excellent reservoir.

The relationship between vertical and horizontal permeability is represented by positive trend with correlation coefficient r = 0.95 which represents an isotropic reservoir (Fig.11).

The permeability porosity relationships for Belayim Formation in Bell Bay – 4 well are shown in Figures (12 & 13) respectively. The linear regression equations and correlation coefficients are represented in

Table (2). The positive trends with highly correlation coefficients (0.87 and 0.91) reflect that, both porosity and permeability are dependant each other.

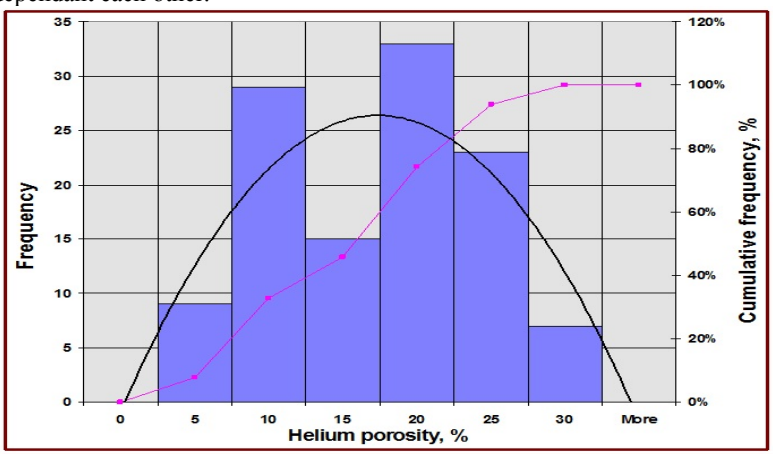

Fig. 8: Histogram and cumulative frequency of helium porosity of Belayim Fm. in BB-4 well.

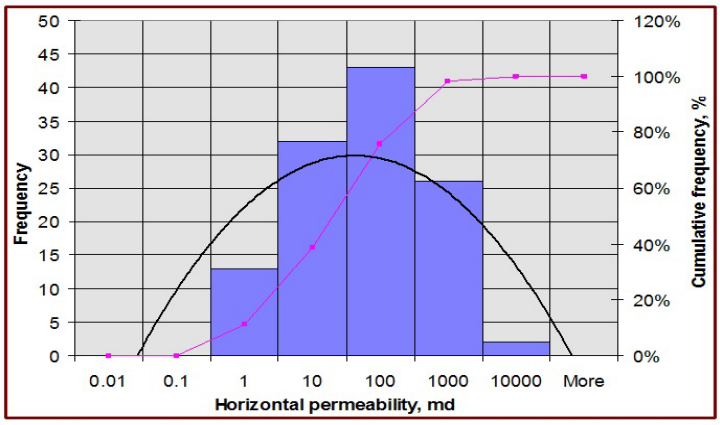

Fig. 9: Histogram and cumulative frequency of horizontal permeanbility of Belayim Fm. in BB-4 well.

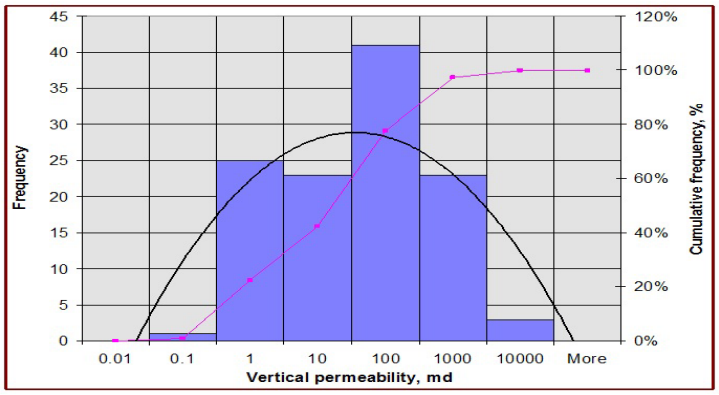

Fig. 10: Histogram and cumulative frequency of vertical permeanbility of Belayim Fm. in BB-4 well.

Table 2: Permeanbility-porosity relationships in Belayim Fm., BB-4 well.

Relation	Linear regression equation	Correlation coefficient (r)	Figure No.
Horizontal permeability with helium porosity	$K_h = 0.3298e^{0.2715\phi_h}$	r=0.87	12
Vertical permeability with helium porosity	$K_v = 0.0926e^{0.3255\phi_h}$	r=0.91	13

The special core analysis defines selected static and dynamic properties of the reservoir. Seventeen core samples are used in this study to illustrate the effect of the pressure on the porosity and the relationship between pore size distribution and pore throat radius in Belayim Formation in Bell Bay – 4 well.

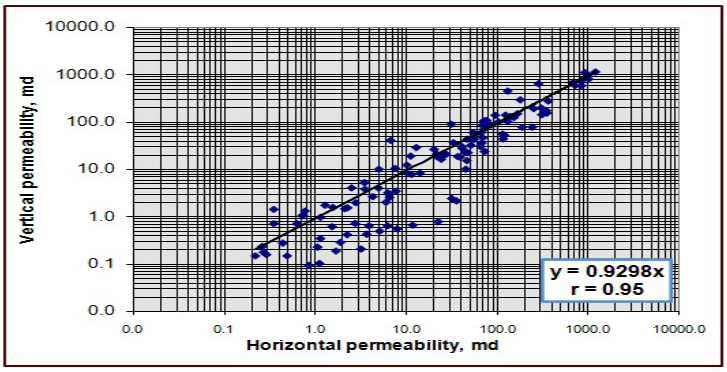

Fig. 11: Relationship between horizontal and vertical permeanbility in Belayim Fm. in BB-4 well.

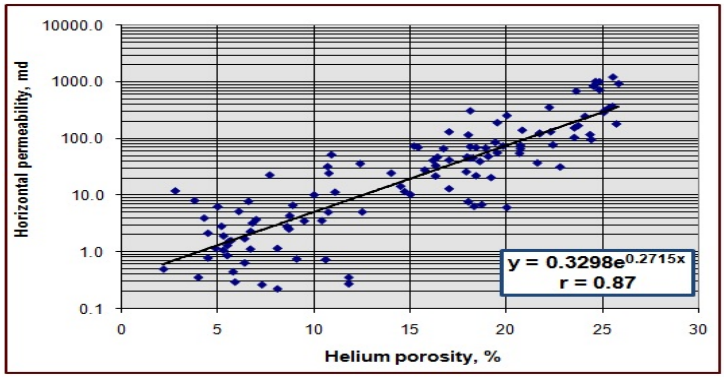

Fig. 12: Relationship between helium porosity and horizontal permeanbility in Belayim Fm. in BB-4 well.

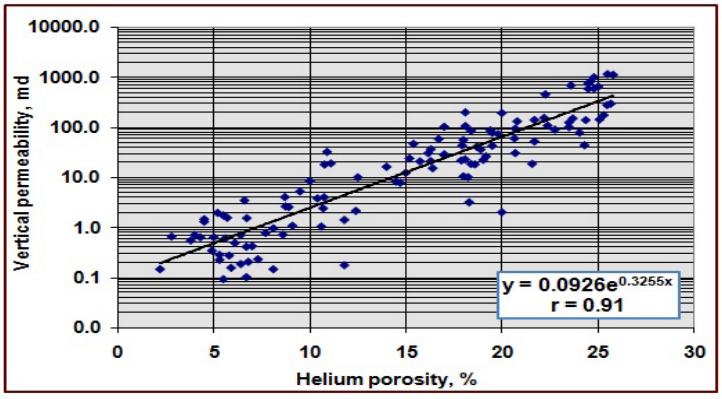

Fig. 13: Relationship between helium porosity and vertical permeanbility in Belayim Fm. in BB-4 well.

Figure (14) illustrates the relationship between the pressure and the porosity for Belayim Formation. The normalized porosity was determined by calculating the average porosity for all samples at the same pressure, the correlation coefficient of this relationship is (-1.0), the very high negative correlation coefficient values indicate that, the porosity correlated reversely with the pressure and the porosity of Belayim Formation could be calculated from the regression equation as

$$\text{Porosity, \%} = 21.848^{*} (\text{pressure})^{-0.0359}$$

Pore size distribution is used to analyze reduction of permeability caused by clay swelling, precipitation of organic matter in pores and growth of microbes in pores (Donaldson *et al*, 1985). Approximate pore size can be obtained from capillary pressure curves by the next equation:

$$Pc = \frac{2\sigma \cos\theta}{r_c} \quad (3)$$

Where: Pc = capillary pressure, σ = interfacial tension,
θ = contact angle and rc = radius of capillary tubes.

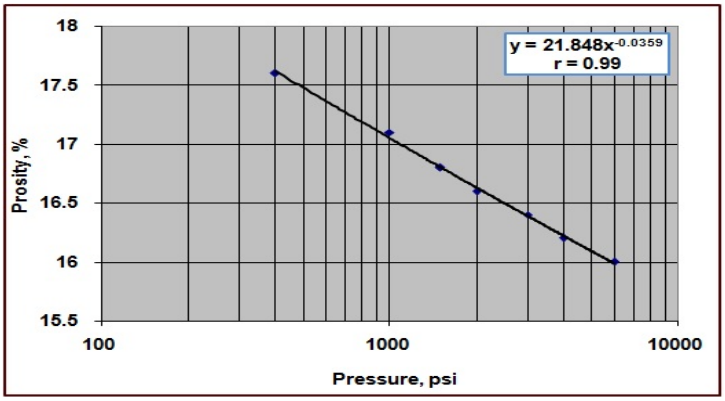

Fig. 14: Relationship between pressure and porosity in Belayim Fm. in BB-4 well.

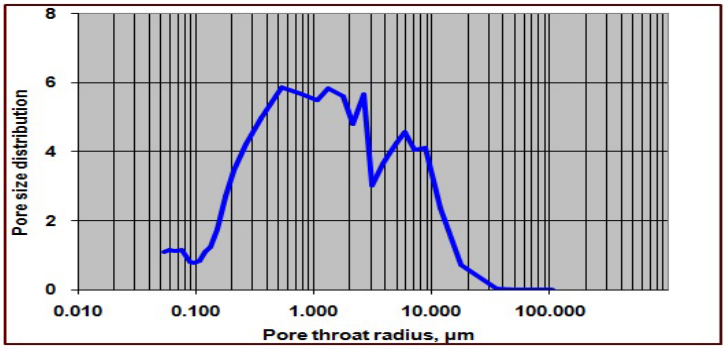

Fig. 15: Relationship between pore throat radius and pore size distribution in Belayim Fm. in BB-4 well.

Diagenetic process and minerals	Eodiagenesis	Mesodiagenesis	Porosity
Compaction	———	———	+/-
Calcite cement	.....	.....	-
Quartz overgrowth	.....	.....	-
Siderite	———	———	+
Pyrite	.....		-
Kaolinite	.....	.....	-
K-feldspar overgrowths		.....	-
Dissolutions of feldspars and micas	.....	.....	-
Ferroan dolomite		———	+

Effective ——— Uneffective .....

Fig. 16: The diagenetic sequence of the Middle Miocene sandstones:, +/- positive / negative influence on development of porosity.

Pore size distribution for 17 samples of Belayim Formation in BB - 4 well were measured at different pore throat radius values (32 values), they are ranging from the minimum pore throat radius (about 0.053µm) to the maximum (17.8 µm). Figure (15) illustrates the relationship between the pore throat radius and the pore size

distribution for Belayim Formation in Bell Bay - 4 well by normalizing all pore size distribution values by calculating the average distribution for all samples. It's clear that the most of pore radii are ranging from 0.3 μm to 10 μm which permit different types of fluid to pass easily indicating relatively high quality reservoir.

Diagenitic History:

There are two stages in the diagenetic history of the Middle Miocene sandstones: eodiagenesis and mesodiagenesis (according to Choquette & Pray, 1970). Eodiagenesis defines early diagenesis, and refers to the period between the end of deposition and the sediment burial to a depth at which the action of surface processes was terminated. Mesodiagenesis corresponds to a period of progressive burial of sediments. A simplified paragenetic sequence of the diagenetic processes in the Middle Miocene sandstones is shown in Figure (16). It was constructed based on petrographic textural relationships, isotopic composition and fluid inclusion of the diagenetic calcite.

Eodiagenesis:

Early deposited sediments have been largely affected by the initial phase of physical compaction, which was progressively accelerated with the increasing depth of burial. The plastic deformation of lithic grains, micas bending and fracture of quartz are the effects of mechanical compaction in the Middle Miocene sandstones (Figs. 6A & E). The effects of this process lead to loss of the rock porosity.

Eodiagenetic siderite and pyrite crystallized when pore water in sediments became significantly depleted in dissolved oxygen. A very fine crystalline form of siderite suggests its early genesis. Siderite precipitated in organic-rich sediments containing significant amounts of reactive iron minerals and in which the pore water was poor in $SO4^{2-}$ (Morad, 1998). According to Mozley (1989), the elemental composition of siderite was controlled by the chemistry of depositional waters. Meteoric siderites were enriched in Mn, but depleted in Ca and particularly Mg in comparison with siderite in the marine sediments. Siderite precipitates from saturated solutions, which are in equilibrium with CO_2 gas or contain a fixed amount of carbonate ions. Another possibility for siderite formation is a bacterial origin, involving the reduction of iron anaerobic sediments (Mason, 2008). Framboidal pyrite formed at the early stage of diagenesis (Fig. 7G). Its existence was connected to local conditions, in which the amount of H_2O produced by sulfate-reducing bacteria was higher than the content of reduced iron (Postma, 1982).

Micrite calcite formed at the early stage of diagenesis. Its precipitation on the surface of grains indicates phreatic or vadose environment (Tucker, 2008). $CaCO_3$ for cement can be sourced internally by the dissolution of metastable carbonate induced by bacterial composition of organic matter, and externally by sea water. Mixing of marine pore water and meteoric ground water could have also caused a supersaturation with respect to calcium carbonate, and could have evoked carbonate precipitation in the mixing zone (Molenaar, 1998).

Silicate grains such as feldspar, micas and rock fragments were altered and dissolved by acidic fluids during eodiagenesis (Fig. 5E). Formation of vermiform kaolinite is attributed to the incursion of meteoric water, which affected mainly mica grains, rarely feldspars (Figs 5E & 7A). Aluminum and silica ions released during the dissolution reaction of detrital grains precipitated as kaolinite in acidic environment (Bjyrlykke, 1989). Kaolinite formation probably predated the quartz cement.

Quartz overgrowths on the quartz grains start to form at the end of eodiagenesis (Figs 5A, 6A & 7F). The meteoric water containing silica, dissolution of detrital feldspar grains and transformation to kaolinite were the most important source of silica for the quartz cement in the early diagenesis.

Mesodiagenesis:

Quartz overgrowths formation was continued. Replacement of quartz and feldspar by carbonates could have a significant importance as silica source for quartz cement at greater depth. As well as, the possible additional source of silica was dissolution of K-feldspar during burial diagenesis (Kozfowska *et al.*, 2011). Quartz cement was strongly affected by temperature as its increase accelerates the rate of cementation (Oelkers *et al.*, 1996).

Locally, blocky kaolinite replaced of vermicular kaolinite. It is the result of dissolution-crystallization reaction involved by the replacement of vermiform crystals by blocky ones (Ehrenberg *et al.*, 1993).

The K-feldspar overgrowths on detrital feldspar grains postdated quartz overgrowths and predated calcite cement (Fig. 6F). K-feldspar precipitation requires high silica activities and high K^+/H^+ ratios (Morad *et al.,* 2000). Residual brines were the possible source for K^+ in the Middle Miocene sandstones. Additional brines were normally acidic and thus capable of dissolving detrital feldspar (Rossi *et al.*, 2002).

Dolomite rhombohedrons postdated quartz overgrowths and predated calcite cement in the studied sandstones (Figs 6B & D). Rhombohedrons of dolomite indicate that, these minerals have been formed through direct precipitation from porewaters (De Souza *et al.,* 1995). The source of the cations Mg^{2+}, Fe^{2+}, Mn^{2+} and Ca^{2+} for carbonates in mesodiagenesis could have been the transformation of detrital clay minerals in the clay rocks (Boles and Franks, 1979). Additional dolomite could have precipitated from brines of high concentration

and high Mg/Ca ratios (Rossi *et al.*, 2002). Calcite cementation, which began in eodiagenesis, continued during mesodiagenesis.

Conclusions:

The Middle Miocene sandstones of Belayim Formation represent fine to coarse grained, angular to subrounded and moderately to poorly sorted sandstone. The detrital framework constituents of the Middle Miocene sandstones are dominated by quartz, feldspar, subordinated lithic fragments and micas. The cement types recognized in the present study include dominant: Fe-calcite, quartz overgrowths, ferroan dolomite, siderite and k-feldspar overgrowth.

The study of the microfacies associations in the Belayim Formation in well Bell Bay– 4 revealed the presence of six microfacies types namely: sideritic subfeldspathic arenite, sideritic quartz arenite, subfeldspathic arenite, sideritic sublithic arenite, sublithic arenite and dolomitic sublithic arenite.

Porosity evolution and quantitative estimation of the amounts of porosity loss by compaction and cementation were obtained from point-count data on cement and pore space abundance. The packing between grains is low to medium. The degree of compaction of these sediments is generally moderate to high, evidenced by concavo-convex and tangential grain-grain contacts.

Diagenetic phenomena have played an important role on the reservoir's petrophysical characterization. The authigenic cement phase is quartz overgrowth cement (up to 3.5 by volume). Late stage siderite cements (up to 23% by volume) and dolomite/ferroan dolomite (up to 26% by volme) are present and these minerals infill intergranular porosity. Localy at depth 2497.23m, they occur as scattered microcrystalline crystals in the sandstones and reduce porosity and probably permeability.

Authigenic clay minerals are represented by kaolinite and grain coating by clay minerals. Kaolinite occurs as booklet and vermicular forms. Primary porosity forms up to 26% and secondary porosity (up to 12%) is also present. The carbonates cementation, quartz overgrowths, dolomitization, mechanical and chemical compaction played an important role of porosity loss in some of the examined samples in the Belayim Formation sandstones.

The reservoir properties of sandstones are controlled by depositional facies, detrital composition, influx of meteoric waters and the depth of burial reached by the sandstones. Evolution path ways of diagenetic and related reservoir properties of the Middle Miocene sandstones have been accomplished during eo- and mesodiagenesis.

The eodiagenesis includes mechanical compaction, pyrite, siderite, dissolution of feldspar and micas grains, micrite calcite cementation, crystallization of kaolinite and quartz overgrowths. The mesodiagenesis includes quartz and k-feldspar overgrowths, crystallization of dolomite/ferroan dolomite and, poikilotopic calcite cementation, dissolution of feldspar grains and calcite cement.

The petrophysical characteristics of the rocks showed that, the sandstones in the Belayim Formation have a high porosity (good to very good) and good to excellent permeability and thus, have a good storage capacity and reservoir quality. The distribution of porosity and permeability values reflects the heterogeneity. The high permeability values, both horizontal and vertical (more than 61 % and 57 %), with relative increasing in horizontal than vertical permeability indicate good reservoir characteristics.

The most of pore radii are ranging from 0.3 µm to 10 µm which permit different types of fluid to pass easily indicating high quality reservoir. The porosity of Belayim Formation strongly correlated reversely with the pressure. The porosity values were coinciding with the effect of authigenic minerals, where observed increasing in siderite and ferroan dolomite accompanied with observed porosity decrease at depths 2497.2m and 2609.9m.

REFERENCES

Bjyrlykke, K., 1989. Sedimentology and petroleum geology. Springer Verlag, Berlin, pp: 363.

Boles, J.R. and S.G. Franks, 1979. Clay diagenesis in Wilcox sandstones of South West Texas: implications of smectite diagenesis on sandstones cementation. Jounal of sedimentary petrology, 49: 55-70.

Choquette, P.W. and L.C. Pray, 1970. Geologic nomenclature and classification of porosity in sedimentary carbonates. AAPG Bulletin, 54: 207-220.

Darwish, M. and M. El-Arabi, 1993. Contributions to the Miocene sequences along the western coast of the Gulf of Suez , Egypt . Egy. Jour. Geol., 37(1): 21-47.

De Souza, R.S., L.F. De Ros, S. Morad, 1995. Dolomite diagenesis and porosity preservation in lithic reservoirs: Carmópolis Member, Sergipe – Alagoas Basin, North Eastern Brazil. AAPG Bull., 79: 725-748.

Donaldson, E.C., G.V. Chilingarian, T.F. Yen, 1985. Enhanced oil recovery, I-Fundamentals and analyses. Elsevier science publ., Amsterdam, pp: 357.

Egyptian General Petroleum Corporation, 1996. Oligocene and Miocene stratigraphy of the Gulf of Suez region. Report, Stratigraphic Committee, pp: 142.

Ehrenberg, S.N., P. Aagaard, M.J. Wilson, A.R. Fraser and D.M.L. Duthie, 1993. Depth-dependent transformation of kaolinite to dickite in sand stones of the Norwegian continental shelf. Clay minerals, 28: 325-352.

El-Gezeery, M.N. and I.M. Marzouk, 1974. Miocene rock stratigraphy of Egypt. Stratigraphic sub-committee of the National Committee of geological science, Egypt. Jour. Geol., 18(1): 1-69.

Ghorab, M.A., 1964. Oligocene and Miocene rock stratigraphy of the Gulf of Suez region, unpublished report consultatus stratigraphic committee of the EGPC., Cairo, E.R., pp: 275.

Jenyon, M.K., 1990. Oil and gas traps. Aspects of their seismostratigraphy, morphology and development. John Wiley and Sons, Chichester, pp: 398.

Kozfowska, A., M. Kuberska, P. Lis and A. Maliszewska, 2011. Diagenesis and reservoir properties of the Middle Miocene sandstones in the Polish segment of the Carpathian Foredeep. Annales Societatis Geologorum Poloniae, 81: 87-103.

Levorsen, A.I., 1967. Geology of petroleum, 2nd edition, W. H. Freeman and Company, San Francisco, pp: 350.

Mason, G.M., 2008. Eocene Age fossilized filamentous bacteria: new evidence suggesting a bacterial genesis of siderite in the Green River Formation. Wyoming, 28th oil shale symposium, Colorado school of mines, 13-15 October: 1-7.

Molenaar, N., 1998. Origin of low-permeability calcite-cemented lenses in shallow marine sandstones and CaCO3 cementation mechanisms, an example from the Lower Jurassic Luxemburg sandstones, Luxemburg. In: Morad, S. (ed.), carbonate cementation in sandstones. International association of sedimentologists, special publication, 26: 193-211.

Morad, S., 1998. Carbonate cementation in sandstones, distribution patterns and geochemical evolution. In: Morad, S. (ed.), Carbonate cementation in sandstones. International association of sedimentologists, special publication, 26: 1-26.

Morad, S., J.M. Ketzer and F. De Ros, 2000. Spatial and temporal distribution of diagenetic alteration in siliciclastic rocks: implications for mass transfer in sedimentary basins. Sedimentology, 41: 1253-1272.

Mozley, P.S., 1989. Relation between depositional environment and the elemental composition of early diagenetic siderite. Geology, 17: 704-706.

Oelkers, E.H., P.A. BjÝrkum and W.M. Murphy, 1996. A petrographic and computational investigation of quartz cementation and porosity reduction in North Sea sandstones, American Journal of Science, 296: 420-452.

Pettijohn, F.J., P.E. Potter and R. Siever, 1972. Sand and sandstone. Springer Verlag, New York, pp: 618.

Postma, D., 1982. Pyrite and siderite formation in brackish and fresh water swamp sediments. American Journal of Science, 282: 1151-1183.

Rossi, C., O. Kälin, J. Arribas and A. Tortosa, 2002. Diagenesis, provenance and reservoir quality of Triassic TAGI sandstones from Ourhoud field, Berkine (Ghadames) Basin, Algeria. Marine and petroleum geology, 19: 117-142.

Tucker, M.E., 2008. Sedimentary petrology. Blackwell, Oxford, pp: 262.